Advances in Science and Technology Research Journal

Advances in Science and Technology Research Journal, 2025, 19(2), 365–382
https://doi.org/10.12913/22998624/196706
ISSN 2299-8624, License CC-BY 4.0

Received: 2024.11.05
Accepted: 2024.12.15
Published: 2025.01.01

Application of machine learning algorithms for recognizing the wear of the cutting tool during precision milling of hardened tool steel

Paweł Twardowski[1*], Maciej Tabaszewski[2], Mateusz Tabaszewski[3], Jakub Czyżycki[1]

[1] Institute of Mechanical Technology Poznan University of Technology, The Faculty of Mechanical Engineering, Pl. Marii Skłodowskiej-Curie 5, 60-965 Poznań, Poland
[2] Institute of Technical Mechanics The Faculty of Mechanical Engineering, Poznan University of Technology, Pl. Marii Skłodowskiej-Curie 5, 60-965 Poznań, Poland
[3] Student at the Faculty of Computing and Telecommunications, Poznan University of Technology, Pl. Marii Skłodowskiej-Curie 5, 60-965 Poznań, Poland
* Corresponding author's e-mail: pawel.twardowski@put,poznan.pl

ABSTRACT

The paper presents extensive research on tool wear and the analysis of diagnostic measures for different cutting speeds (v_c). The work is divided into two parts. The first part involves conducting an experiment on a machining center, measuring the tool wear index, and recording vibration acceleration signals, followed by analyzing the obtained results. In the second part, the authors focus on determining appropriate diagnostic signal measures and their selection and applying various machine learning methods. The machine learning pertains to classifying the tool condition as operational or non-operational. The best of the tested classifiers achieved an accuracy of 0.999. Thanks to the comparative analysis, it was possible to propose a condition monitoring method that is based only on vibration acceleration without taking into account the cutting speed parameter. Vibration measurement can be performed on the spindle. In this case, the weighted accuracy value determined on the test set was 0.993. The F1 coefficient characterizing both precision and accuracy was 0.982. The authors consider this result to be satisfactory in industrial conditions. Measurement on the spindle without the need to take into account the cutting speed is easy to use in industrial practice

Keywords: milling, hardened steel, tool wear, diagnostics, machine learning.

INTRODUCTION

The most important aspect of diagnostics in the cutting process is recognizing the degree of tool wear. Tool wear often occurs randomly and is one of the most complex phenomena in the cutting process. It can lead to consequences such as damage to the workpiece or even damage to the machine tool. The tool wear process is cyclical, and the duration of a single wear cycle is relatively short.

Various physical phenomena inherently linked to the cutting process are used for tool diagnostics. Tool wear is associated with an increase in cutting forces, the current drawn by the drive motor, acoustic emission, mechanical vibrations, temperature, noise levels, etc. Often, these relationships are non-monotonic, and subtle geometric changes in the tool frequently determine the momentary increase or decrease in the physical quantities. All of this affects not only the tool's durability but also the technological effects and accuracy of the process.

Therefore, the diagnostics of the cutting process involves measuring signals of one (or several simultaneously) of the aforementioned quantities

and, based on their appropriate measures, obtaining information about the state of the tool or the process in general. The key to achieving this goal is the use of appropriate measurement sensors and diagnostic inference models. Modern inference models often rely on machine learning, achieving high efficiency. The authors of the study [1] analyzed the frequency of using artificial intelligence methods in 56 articles published over the last 10 years (in this journal) concerning milling processes. The most frequently published articles were about artificial neural networks, followed by the hidden Markov model, support vector machines, principal component analysis, C-means clustering, K-star, relevance vector machines, extreme learning machines, and others. Their common feature was that the input data for the diagnostic model came from sensors measuring the physical phenomena accompanying the cutting process.

In monitoring the cutting process, the most commonly used signals are cutting forces [2–4], vibrations [5–7], and acoustic emission [8–12]. After determining the appropriate measures, the input data is processed by a suitable diagnostic model based on artificial intelligence. Currently, the most popular artificial intelligence methods include neural networks (NN), image recognition (IR), fuzzy logic (FL) and the evolution of fuzzy rules, adaptive neuro-fuzzy inference systems (ANFIS), Bayesian networks, support vector machines (SVM), decision and regression trees, k-nearest neighbors algorithm (kNN), hidden Markov model (HMM), singular spectrum analysis (SSA), and genetic algorithms (GA) [13].

Many machine learning methods can be applied to solve the problem of diagnosing the technical condition, including the state of the tool [14]. Each of them has its pros and cons. It is important to remember that there is no single method that provides the best results for every data set, hence the necessity to compare several before making the final choice of algorithm. It is worth mentioning some of them due to their application in the later part of this work.

One of the most popular machine learning (artificial intelligence AI) techniques is neural networks. Their most important advantage is their ability to generalize and highlight hidden relationships between input and output data [15, 16]. Neural networks are successfully used in both direct and indirect measurements of tool wear. Moreover, they can be applied to any cutting method such as turning [17, 18], milling [19, 20], grinding [21], etc. Sometimes hybrid models are used, as in the study [22]. The proposed hybrid model provided very good results in determining progressive tool wear. During milling, a deep convolutional neural network was used to analyze data from vibration and cutting force sensors. Experimental studies showed that the proposed method is significantly better than other advanced methods. The only drawback of neural networks is the need for a sufficiently large dataset to achieve the highest efficiency. In industrial applications, this condition is not always easy to meet.

Another popular machine learning technique is decision trees, which are most often used for classification. Decision trees can handle both categorical and numerical data. A major advantage of classification trees is the easy and straightforward interpretation of results by humans (white-box model), which can be presented as a set of classification rules. These rules can be easily implemented in automated supervision systems. Another advantage is the lack of necessity for feature selection, as features are automatically selected during the comparison of quality measures at a given tree node. However, drawbacks include susceptibility to overfitting, sensitivity to the rotation of the training set, and generally high sensitivity to changes in the training set [23].

An important group of machine learning methods is ensemble learning, including random forests. Predictions are made based on the voting of many independent trees. It has been shown that even a set of weak independent classifiers, which perform only slightly better than random guessing, can, through voting, provide very accurate predictions. The independence of individual trees is achieved by randomly selecting subsets of features based on which the individual trees are built, which reduces the variance of the overall model [24].

The k-nearest neighbors (kNN) method is an algorithm that classifies an entry based on its nearest neighbors. This technique is quite effective in labeling unidentified input data. The kNN method is used in a number of machine learning tasks, such as computer vision and handwriting recognition [13]. The method is simple to interpret and boils down to determining the nearest neighbors of the recognized vector based on a chosen distance measure [25]. However, the drawback is the lack of a generalizing model and the need to

calculate the distance measure from all training patterns, which is associated with relatively long computation times.

The practical application of machine learning in cutting processes aims to determine the state of the tool cutting edge as either usable or unusable. Thus, it is a classification task. In autonomous machining centers, the basic information needed is whether the tool should be replaced with a new one or if it can still be used. The classification process involves processing data from measurement sensors, determining signal measures and based on machine learning, deciding whether the tool is usable or not.

This work aims to apply machine learning algorithms to recognize the state of the tool during the precision milling of hardened tool steel. To this end, the method of selecting measures and their use in machine learning is presented. An essential part of the work is also the procedure for minimizing input data while maintaining the assumed effectiveness of the inference system. The results of the work can be used to build an effective diagnostic system.

SCOPE OF RESEARCH

The research was conducted on a 3-axis high-speed milling center, DMC70V hi-dyn, with a Heidenhain TNC 426M controller, equipped with a spindle with a maximum rotational speed of n = 30.000 rpm.

The workpiece material used was hot-worked alloy tool steel 55NiCrMoV7 with a hardness of 50 HRC. The chemical composition of the steel is provided in Table 1. The workpiece was in the shape of a rectangular prism with dimensions 200 × 100 × 84 mm, clamped in a machine vise (Fig. 1).

The tool used was a solid toroidal end mill with a diameter of D = 12 mm (corner radius r_ε = 0.5 mm, rake angle γ_f = -5°, number of cutting edges z = 4, helix angle of the main cutting edge λ_s = 55°) from FRAISA, symbol X7200491 (Fig. 2a). The end mill had a TiCN wear-resistant coating and was mounted in a thermal holder from Kelch, Ø12 HSK50E, with the designation 8466100130 (Fig. 2b).

The parameters for milling are presented in Table 2. The research was conducted for six different cutting speeds v_c, while keeping the other parameters constant.

RESEARCH METHODOLOGY

Milling was performed in the climb milling mode over a cutting path L = 200 mm (a single pass along the longest side of the rectangular prism). For each cutting speed v_c, the tool wear was measured after a specified number of passes. The tool wear indicator used was the flank wear

Table 1. Chemical composition of steel 55NiCrMoV7 [26]

C	Mn	Si	P	S	Cr	Mo	Ni	V
0.5–0.6	0.6–0.9	0.1–0.4	< 0.03	< 0.03	0.8–1.2	0.15–0.25	1.5–1.8	0.05–0.15

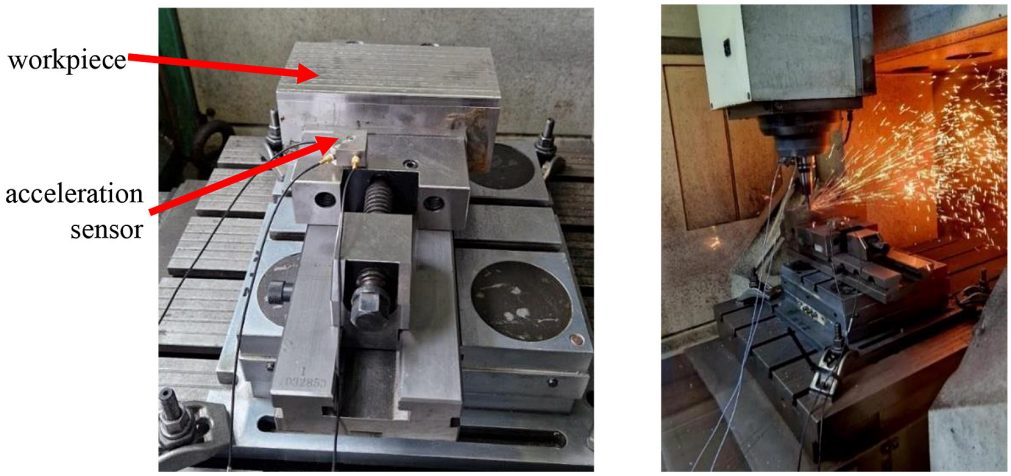

Figure 1. Photo of the clamped sample and view during milling

Figure 2. Solid end mil

Table 2. Milling parameters used in the experiments

Cutting speed v_c [m/min]	300	500	600	700	800	1000
Feed per tooth f_z [mm/tooth]	0.05					
Rotational speed n [rpm]	7962	13270	15924	18577	21231	26540
Feed rate v_f [mm/min]	1592	2654	3185	3715	4246	5308
Radial depth of cut a_e [mm]	0.2					
Axial depth of cut a_p [mm]	2					

width at the corner – *VBc* (Fig. 3). Measurement of *VBc* was conducted using a ZEISS SteREO Discovery V12 stereoscopic microscope (Fig. 4). The flank wear width *VBc* was measured for each of the 4 cutting edges and then the average value was determined.

The number of passes after which tool wear was measured was variable and depended on the current value of the wear indicator. Measurements were most frequently taken after 50 or 100 passes over the path L = 200 mm. The criterion for tool wear was set at:

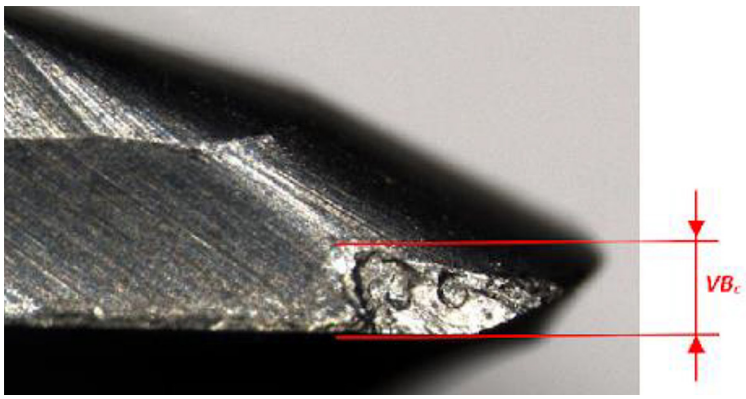

Figure 3. Schematic of the VBc measurement

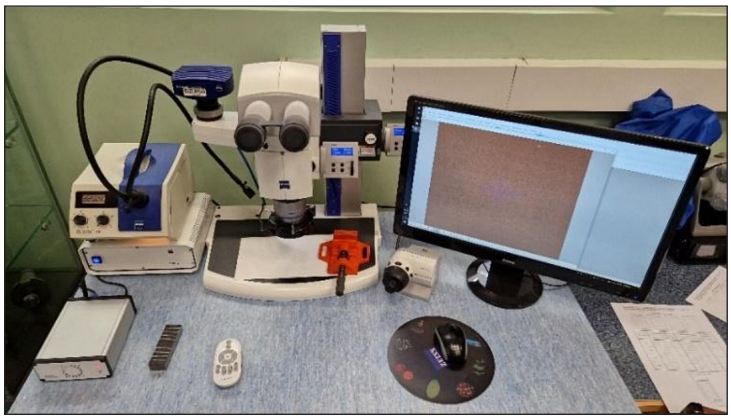

Figure 4. ZEISS Stereo Discovery V12 stereoscopic microscope

$$VBc = 0.3 \text{ mm}$$

In parallel with the tool wear measurements, vibration acceleration measurements were conducted. Piezoelectric sensors from Bruel&Kjaer, model 4321, were used for measuring vibration accelerations. The sensors were mounted on the clamp and spindle using threads. The following directions were analyzed (Fig. 5):

- Channel 1 – sensor mounted on the clamp in the normal feed direction – Cl_A_{fN},
- Channel 2 – sensor mounted on the clamp in the thrust direction – Cl_A_z,
- Channel 3 – sensor mounted on the spindle in the normal feed direction – Sp_A_{fN},
- Channel 4 – Sensor mounted on the spindle in the thrust direction – Sp_A_z.

Figure 6 shows the setup for measuring and analyzing vibration accelerations. Signals from the sensors were transmitted to a NEXUS amplifier from Bruel&Kjaer and then to an analog-to-digital converter. The signals from the converter were recorded by a computer using special software, AnalizatorADV01, with a sample screenshot shown in Figure 7.

The absolute acceleration signals were recorded and sampled synchronously at a frequency of fp = 65536 Hz from four channels of the converter. Such a high-frequency bandwidth allowed for the

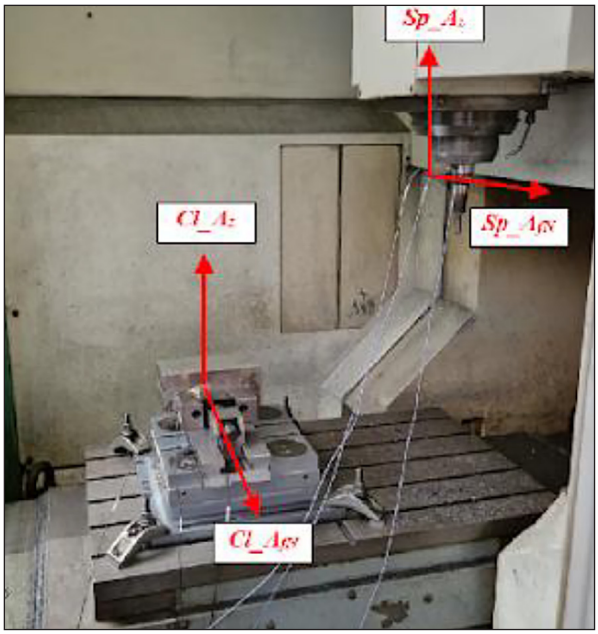

Figure 5. Analyzed vibration directions

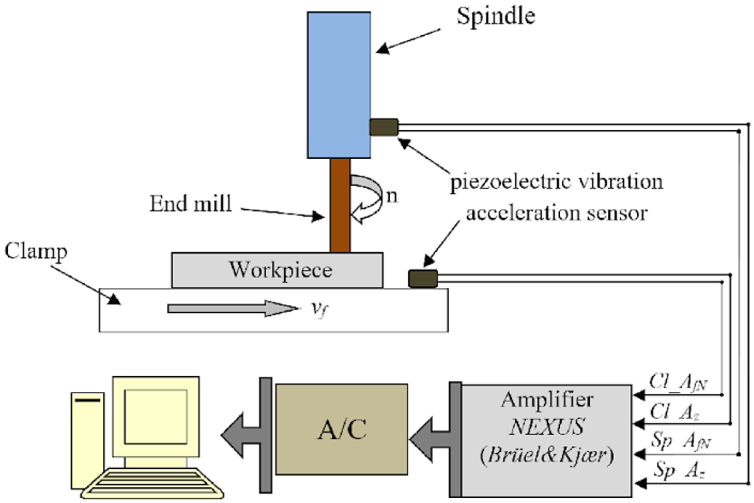

Figure 6. Diagram of the vibration acceleration measurement path

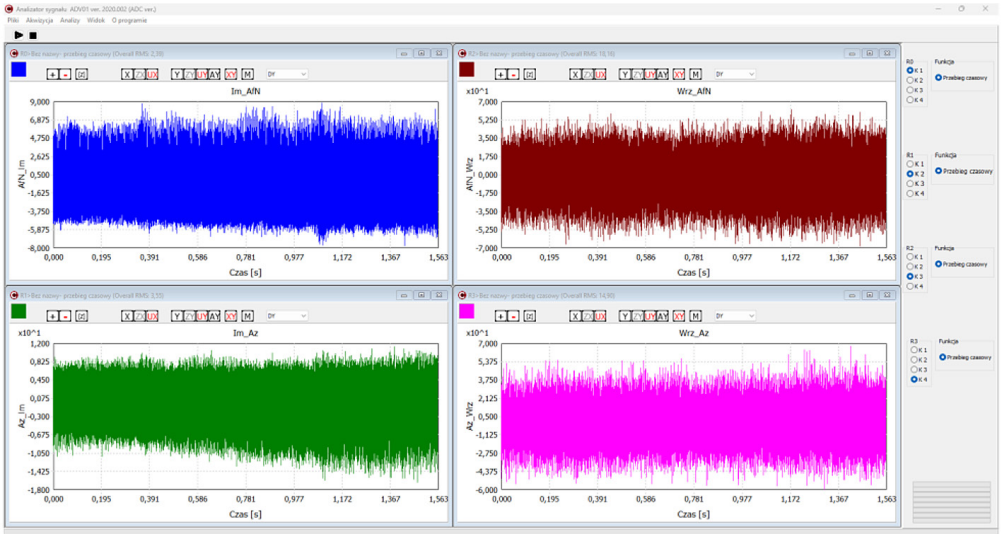

Figure 7. Screenshot of a program for recording and analysis of vibrations: top left window – sensor mounted on the clamp in the normal feed direction, top right window – sensor mounted on the clamp in the thrust direction, bottom left window – sensor mounted on the spindle in the normal feed direction, bottom right window – sensor mounted on the spindle in the thrust direction

potential analysis of phenomena related to friction in accordance with the suggestions contained in [27]. The first two channels covered vibration accelerations recorded on the clamp (in the normal feed direction and radial directions). The next two channels were connected to the acceleration signals recorded in the same directions but from the measurement point on the spindle. The spindle is relatively the least problematic location for sensor mounting in practical production. Unfortunately, the measured vibrations are not only related to the technological process but also to all vibration sources arising within the spindle itself and related to the spindle's drive. On the other hand, placing the vibration transducer on the clamp leads to several issues related to workpiece mounting, risk of cable breakage, potential sensor damage, negative interaction of coolant directly on the sensor, etc. However, the sensor mounted on the clamp seems to be directly closer to the cutting process itself, which, as initially assumed, should allow for a more accurate diagnosis of tool wear.

Figure 8 shows the kinematic and geometric diagram of down milling with the cutting angle ψ. indicated. Knowing the kinematic and geometric parameters of milling, the number of active cutting edges z_c (the number of edges simultaneously cutting) for a helical end mill can be calculated using Equation 1.

$$z_c = \frac{\Psi}{\Psi_z} + \frac{B \cdot z \cdot tg\lambda_s}{\pi \cdot D} \tag{1}$$

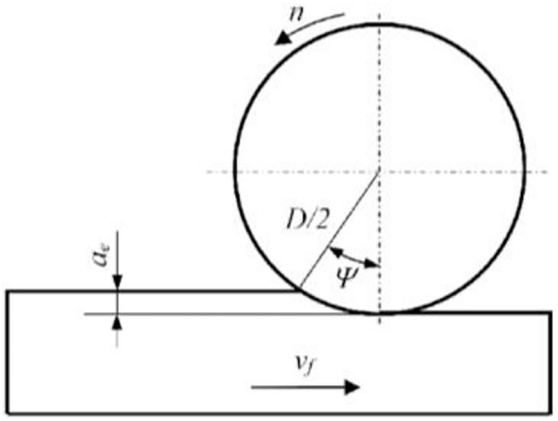

Figure 8. Kinematic and geometric diagram of down milling

where: ψ – cutting angle of the mill; ψ_z – inter-edge spacing angle; B – width of milling $B = a_p$; z – number of cutting edges; λ_s – helix angle of the main cutting edge

$$z_c = \frac{14.8}{90} + \frac{2 \cdot 4 \cdot tg55}{\pi \cdot 12} = 0.47$$

$$z_{c\_min} = 0, z_{c\_max} = 1$$

This means that the maximum number of active cutting edges is 1, while the minimum is 0. This is related to the impulsive nature of the mill's operation, which is clearly visible in the example spectrum shown in Figure 9. For all other cases,

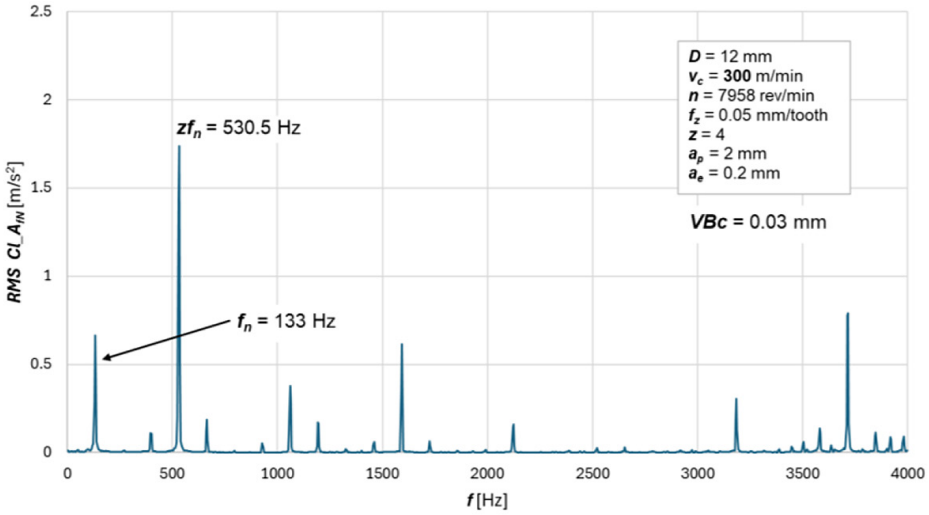

Figure 9. Example spectrum for the sensor mounted in the normal feed direction to the Cl_A_{fN} clamp

the spectrum predominantly featured frequencies related to the kinematics of milling, mainly the component $z{\cdot}f_n$ – the frequency of rotation multiplied by the number of cutting edges.

RESULTS ANALYSIS

Figure 10 presents example images of tool wear for an average *VBc* value of 0.52 mm at a cutting speed of v_c = 700 m/min. The visible damage to the cutting edge in the form of abrasive wear may result from excessive mechanical loads, which can occur when working at too high a cutting speed. Chipping of the cutting edge on the flank surface, characteristic of tool operation under difficult cutting conditions or caused by a sudden impact force, is also noticeable. Similar results were obtained for all other cutting speeds tested. Changes in the *VBc* indicator as a function of cutting time t_c for all tested cutting speeds are shown in Figure 11 Based on these curves (using the wear criterion), the tool life for all cutting speeds can be determined (Figure 12). The longest tool life was obtained at the lowest cutting speed v_c = 300 m/min, amounting to T = 580 min. Achieving the longest life at the lowest cutting speed is expected and consistent with Taylor's tool life equation. Ambiguous results were obtained only for the speeds v_c = 700 m/min and v_c = 800 m/min. The changes in *VBc* as a function of cutting time *tc* are similar, and the differences in tool life are comparable, although a slightly longer life was achieved for v_c = 800 m/min – T = 58 min (v_c = 700 m/min – T = 52 min).

The tool life graph (Figure 12) allows for predicting the tool life for cutting speed ranges that were not tested. For this purpose, the so-called Taylor's equation is ideal, shown in the form $T = C/v_c^s$, where s = 2.88. As tool wear progresses, the intensity of physical phenomena associated with the cutting process increases. With increasing *VBc* indicator, the amplitude of vibration accelerations changes, but this relationship is not monotonic. This means that increased tool wear does not always lead to increased vibration amplitude. The tool wear process involves not only wear on the cutting surface but also wear on the cutting edge surface, micro-chipping of the cutting

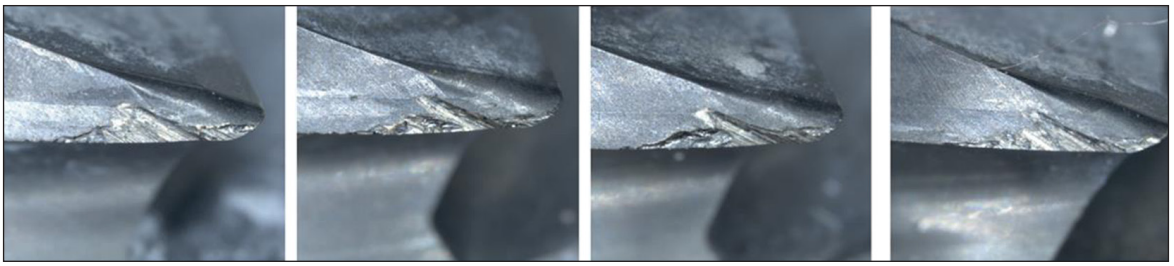

Figure 10. Tool wear images for VBc = 0.52 mm (at v_c = 700 m/min)

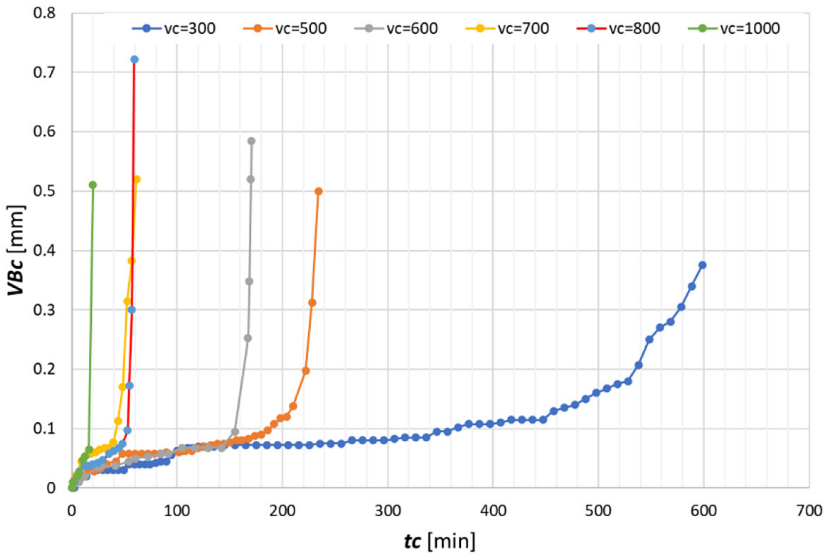

Figure 11. Variation of the VB_c indicator as a function of cutting time t_c for the tested cutting speeds v_c

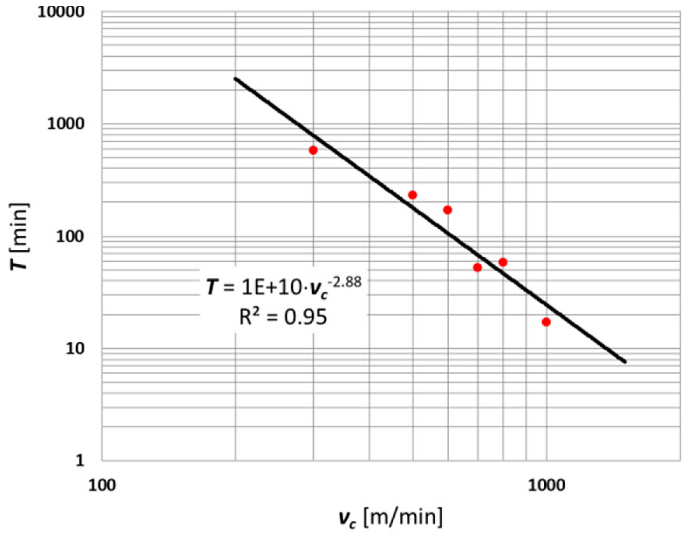

Figure 12. Effect of cutting speed v_c on tool life T

edge, cracks, build-up, etc. These symptoms often occur randomly, resulting in a non-monotonic distribution of vibration measures as a function of tool wear. Figure 13 shows example changes in vibration acceleration as a function of tool wear for a cutting speed of v_c = 800 m/min. Each point on the graph is represented by the root mean square (RMS) value calculated from the vibration data in the time domain. Channels 1–4 were described earlier. The coefficient of determination R^2 is quite high, indicating a good fit of the results to the trend line, but inference based on an explicit mathematical form is fraught with significant uncertainty. Machine learning methods are definitely better suited for this purpose.

APPLICATION OF MACHINE LEARNING METHODS FOR TOOL CONDITION MONITORING

Preprocessing

The initial goal of the analysis was to assess whether measurements taken from the spindle provide acceptable diagnostic accuracy for the tool's condition. Another important issue is the impact of cutting speed on the vibration signal used as input for the tool condition diagnostic system. Obtaining information about the cutting speed requires integration with the machine control system as well as acquiring information from

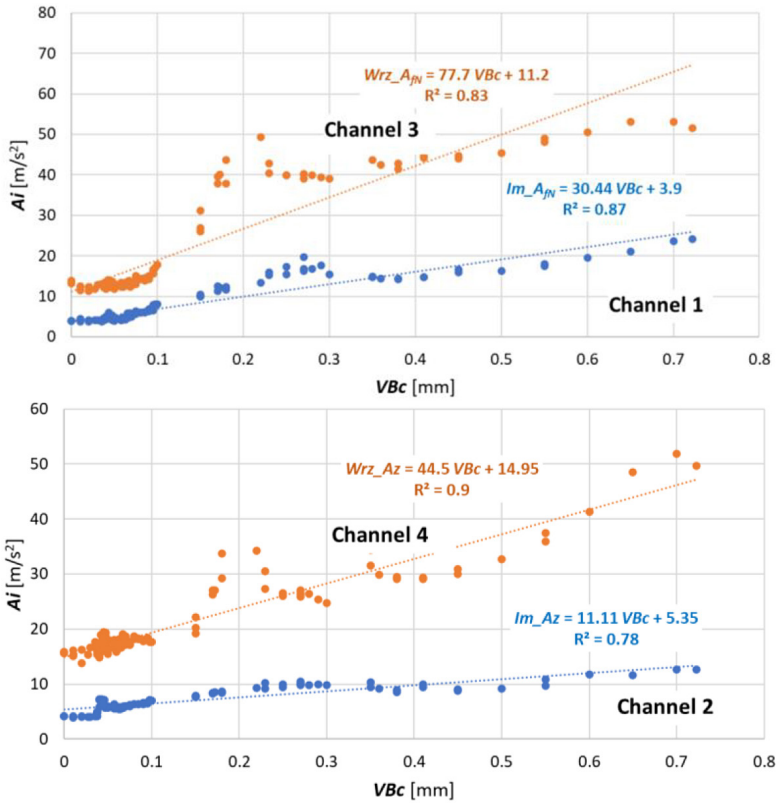

Figure 13. Changes in the root mean square value of vibration accelerations as a function of tool wear for the 4 tested channels and for v_c = 800 m/min

the operator, which in industrial conditions is associated with a significant risk of error. Therefore, another goal of the study was to attempt to eliminate the dependence on cutting speed information from the decision-making process regarding the tool's condition. This approach aims to develop an autonomous diagnostic system that reports the tool condition based solely on vibration signals.

Of course, it should be noted that the conducted tests might not be adequate if the type of tool or the machined material changes. Vibration measurements included a total of 411 recordings, each approximately 1.5 seconds in length. Each recording covered a segment of the signal where the tool was entirely working in the material. For model construction, the fusion of vibration signal recordings and recorded tool wear indicator values (*VBc*) was performed.

Figure 14 illustrates sample fragments of vibration acceleration recordings obtained during the cutting process at a cutting speed of v_c = 300 m/min. In the left column, signals related to the initial stage of tool wear (*VBc* = 0 mm) are shown, while the right column presents advanced tool wear stages (*VBc* = 0.375). The subsequent rows represent measurement points and directions, including clamp - normal feed direction (Cl_A_{fN}), clamp - thrust direction (Cl_A_Z), spindle - normal feed direction (Sp_A_{fN}), and spindle - thrust direction (Sp_A_Z)

Analysis of the sample compilation from Figure 14 and many other comparisons shows that the nature of vibrations recorded on the clamp and spindle is different. The dynamics of signal level changes in both measurement points also vary between new tools and tools with advanced wear. In many cases, changes in vibration levels are most significant in the resistance direction for the clamp and in the feed direction for the spindle. This could be due to the differing stiffness of the system in both directions at various measurement points. Analyzing the example in Figure 14, it seems that simple signal measures such as RMS might be sufficient for determining the tool condition or wear extent. Unfortunately, this view is significantly distorted by varying cutting speeds, which we do not wish to include in the model. Figure 15 shows RMS values across the entire measurement band for all available data.

As can be seen from the analysis in Figure 15, it is necessary to use more advanced methods to build a multiparametric model that assesses tool wear based solely on vibration signals without considering cutting speed v_c. The first approach

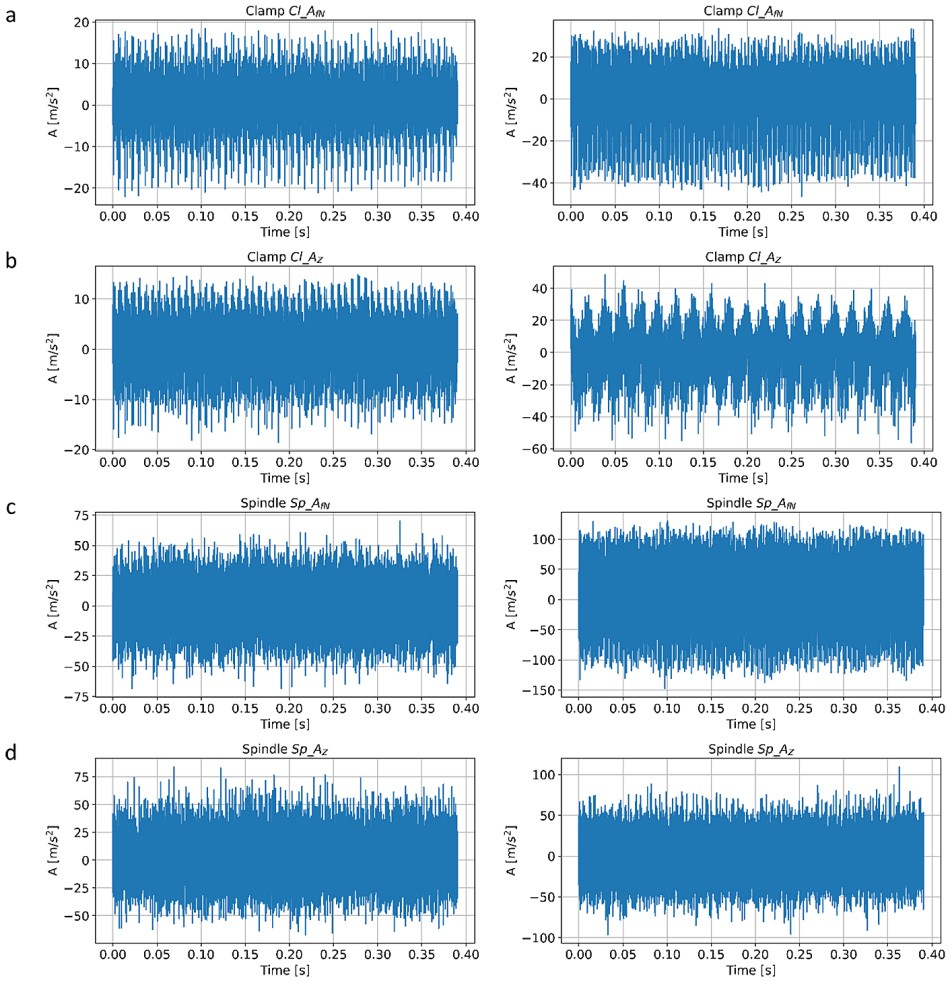

Figure 14. Compilation of sample segments of vibration signal recordings for the cutting process at v_c = 300 m/min. In the left column – new tool, in the right column – tool after reaching VBc = 0.375 mm. Rows: a) clamp – normal feed direction (Cl_A_{fN}), b) clamp-thrust direction(Cl_A_Z), c) spindle – normal feed direction (Sp_A_{fN}), and d) spindle-thrust direction (Sp_A_Z)

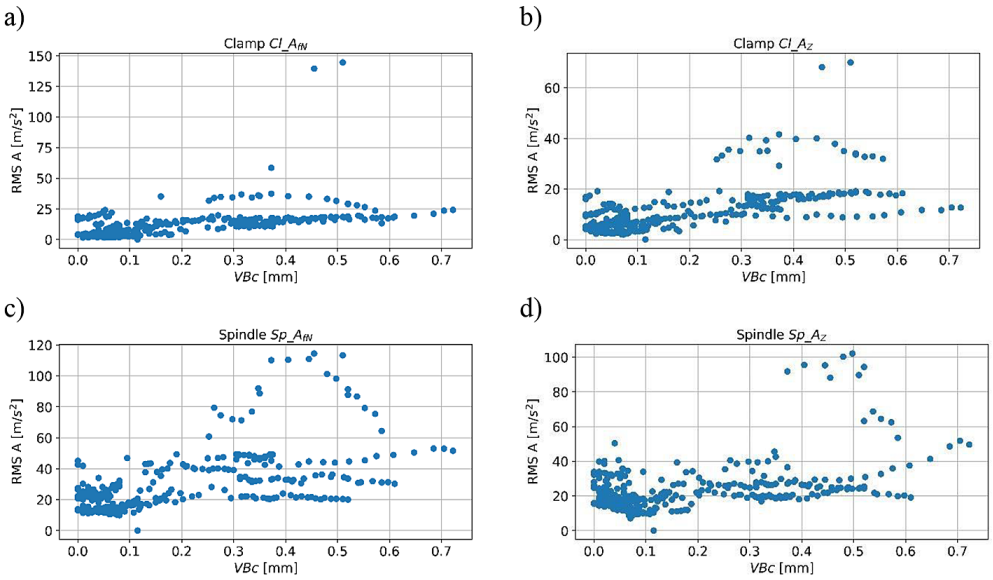

Figure 15. Effective values of vibration accelerations as a function of the wear indicator VBc for all available data.

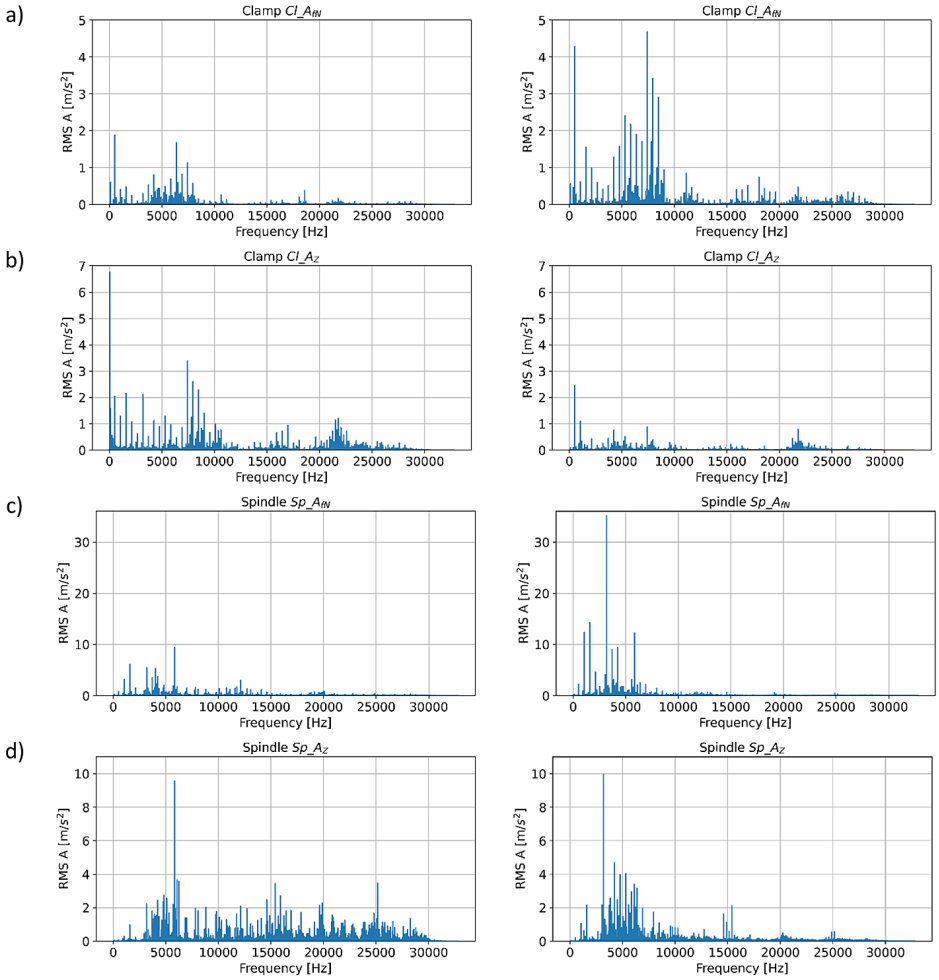

Figure 16. Comparison of sample frequency domain analysis results of the vibration signal for the cutting process at v_c = 300 m/min. Analyses pertain to signals from Figure 14

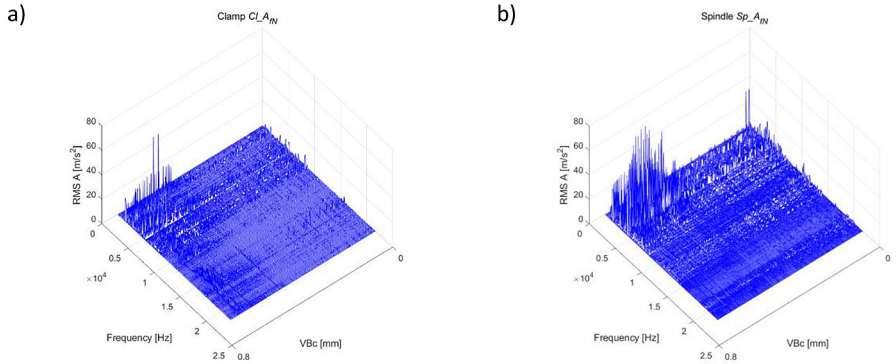

Figure 17. The cascading plot of RMS values was determined in 100 Hz bands. Results are ordered by increasing VBc. The plot includes all examples from different cutting speeds. Figures a) measurement point on the clamp, b) on the spindle

involved attempting to isolate frequency bands that might allow a selective choice of diagnostic measures. Figure 16 presents the results of frequency domain analysis for the same example signals shown in Figure 14.

The comparison of the spectra presented in Figure 16 suggests that crucial information about tool wear changes often lies in narrow frequency bands, which typically differ for various measurement points. Sometimes these changes are not

straightforward; for instance, in Figure 15d, the dominant component for the new tool decreased with increasing wear, while another component became dominant. To identify active frequency bands and extract those containing information about tool wear, cascading plots were created showing RMS values of vibration accelerations in bands of an arbitrarily chosen width of 100 Hz for all available recordings. The results were ordered by progressing wear measured by *VBc*. RMS values in bands were calculated from spectral analysis results. Sample comparisons for the feed direction and measurement points on the clamp and spindle are shown in Figure 17.

The conducted analysis allowed extracting information about significant frequency bands related to changes with wear progression. The assumption is that replacing wide-band analyses with narrow-band analyses should enhance sensitivity. Another preliminary data selection attempt involved singular spectrum analysis (SSA) [28]. This method was chosen because of its capability to extract only the most significant information from the vibration signal. SSA is used for decomposition, trend extraction, periodicity detection and extraction, filtering, denoising, and forecasting. A time series signal can be the sum of many components, including noise. SSA analysis can isolate the most critical components of the signal for separate consideration. The SSA component extraction algorithm starts with using a given time series $Y_T = (y_1, y_2, \ldots y_T)$ cto determine the trajectory matrix:

$$X = \begin{bmatrix} y_1\, y_2 & \cdots & y_{T-L+1}\, y_2\, y_3 & \cdots \\ y_{T-L+2} & \cdots & \cdots & \cdots \cdots\, y_L\, y_{L+1} \cdots\, y_T \end{bmatrix} \quad (2)$$

where: L is the time window width.

This way the time series is divided into overlapping segments. In the next step, SVD decomposition was applied to determine the Eigenvalues and Eigenvectors of the Matrix XX^T [28-30]. Matrix X can be defined as:

$$X = \sum_{i=1}^{d} \sqrt{\lambda_i} u_i v_i^T = \sum_{i=1}^{d} X_i \quad (3)$$

where: $\lambda_1 \geq \lambda_2 \ldots \geq \lambda_L \geq 0$ and $u_1, u_2 \ldots u_L$ are respectively eigenvalues and eigenvectors of the matrix XX^T, $v_i = X^T u_i / \sqrt{\lambda_i}$, d = $max\{i \in \{1, \ldots, L\}: \lambda_i > 0\}$ X_i define elementary matrices.

In the next stage, a group of l eigenvectors ($1 \leq l \leq L$) is selected. To do this, the entire set of indices i {1, 2, ... d} is divided into disjoint subsets $L = \{i_1, i_2 \ldots i_p\}$. For a given group, it can be written as:

$$X_L = \sum_{j \epsilon L} \sqrt{\lambda_j} u_j v_j^T \quad (4)$$

The final step of the algorithm involves reconstructing the time series, which serves as an approximation Y. This is done by diagonal averaging each X_L to obtain subsequent components. The resulting components of the time series can be used for further analysis.

Sample fragments of recordings obtained on the spindle in the feed direction during the initial phase of tool operation and after reaching wear $VB_c \approx 0.1$ mm, along with their distributions on the three most important components, are shown in Figure 18.

Although, as shown in the figures, the most significant information is concentrated in the first principal component, the results of the proposed transformation were still used. It was assumed that during the model training phase, methods that automatically select the most relevant features for classification or regression (e.g., decision trees or random forests) would utilize measures based on different components. If the

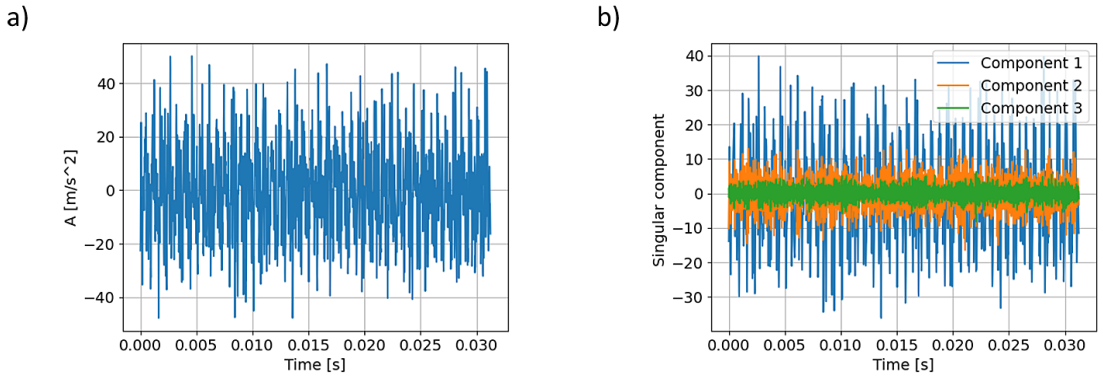

Figure 18. a) Example of vibration acceleration signal recorded during the experiment, b) Example of the three components obtained using SSA

essential diagnostic information is contained in the first components, then excluding the others, considered as noise, may improve the model's quality. On the other hand, further components obtained through SSA may be related to more subtle changes in signal characteristics, which might omit phenomena related to, for example, process kinematics that might not carry diagnostically useful information. Thus, the proposed analysis was deemed justified.

Classification of tool condition using machine learning methods and results

To build the classifier, it was assumed that a value of VBc = 0.35 mm distinguishes between a usable and unusable tool. Measures of vibration signals were considered in full band of frequency and separately in filtered bands (see Table 3). It was also taken into account the most important components obtained through SSA (for full band signals). Vibration signals were recorded on the spindle and vice in the feed and radial directions. The following measures were determined (for vibration signals and SSA components), which were the input to the various classification models: effective value (RMS), peak value, mean peak value from several realizations, average signal value, root amplitude, peak factor, shape factor, clearance factor, impulsivity factor, kurtosis, skewness, and Rice frequency. Definitions of the applied measures can be found in [27]. Several classifier algorithms were used to compare results, based on the principle that there is no single best method for all types of data. These included: binary classification and regression trees (CART), random forests, nearest neighbor classifiers, and a Multi-Layer Perceptron (MLP) neural network with a softmax output layer. Deep learning methods were not considered due to the small number of examples. Before building the model, the data was normalized and centered. To determine the best model, training and test sets were created -see Figure 19. Comparative analyses were conducted based on the training set, with hyperparameter tuning performed using 5-fold cross-validation (CV) and mean squared error (MSE). The models used and the changed hyperparameters tested using cross-validation are listed below:

- CART decision tree; hyperparameters: max depth of the tree (in the range from 2 to 20), split criterion (entropy and Gini index)
- k-Nearest neighbors algorithm; hyperparameters: k neighbors (in the range from 1 to 20), distance metric (euclidian, city-block)

Table 3. Selected frequency bands based on previously presented analyses

Signals	Included measures			
Signals over the entire measurement range from the feed and radial directions measured on the clamp and spindle. In total, 48 parameters for 4 channels.	1. 2. 3. 4. 5. 6.	rms, peak, mean_peak, avg, root, CF,	7. 8. 9. 10. 11. 12.	FF, CLF, IF, kurtosis, skewness, Rice_f
Filtered signals in bands from the feed and radial directions measured on the clamp and spindle. In total, 156 parameters.	13. 14. 15. 16. 17. 18.	rms, peak, mean_peak, avg, root, CF,	19. 20. 21. 22. 23. 24.	FF, CLF, IF, kurtosis, skewness, Rice_f
	In bands: *for the clamp*		In bands: *for the spindle*	
	25. 26. 27. 28. 29. 30. 31. 32. 33.	Cl_A_{fN} 2 – 2.5 kHz, Cl_A_{fN} 3 - 4 kHz, Cl_A_{fN} 4 – 4.5 kHz, Cl_A_{fN} 5 – 5.5 kHz, Cl_A_{fN} 7 – 7.5 kHz; *Cl_Az* 2 – 2.5 kHz, *Cl_Az* 4 – 4.5 kHz, *Cl_Az* 8 - 9 kHz, *Cl_Az* 9.5 – 10 kHz	34. 35. 36. 37.	Sp_A_{fN} 3 – 3.5 Hz, Sp_A_{fN} 4 – 4.5 Hz, Sp_A_{fN} 5.5 – 6.5 Hz; *Sp_Az* 3.5 - 5 Hz
Particular components obtained after SSA decomposition of the signal from the feed and radial directions measured on the clamp and spindle. In total, 144 parameters.	38. 39. 40. 41. 42. 43.	rms, peak, mean_peak, avg, root, CF,	44. 45. 46. 47. 48. 49.	FF, CLF, IF, kurtosis, skewness, Rice_f

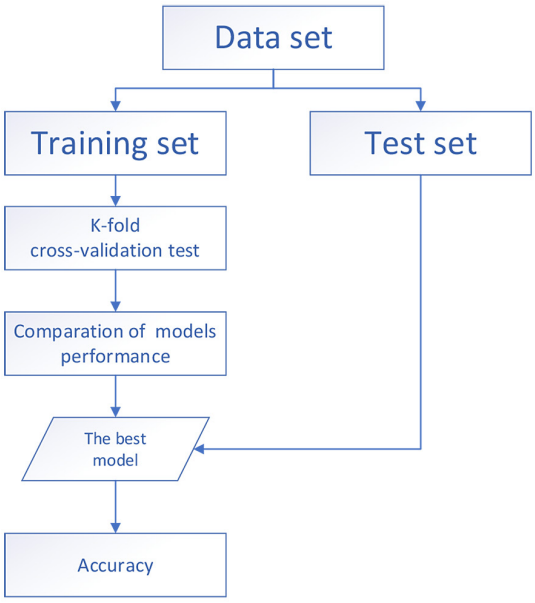

Figure 19. Algorithm for building models based on data subsets

- Random forrest; Hyperparameters: number of estimators (from 20 to 80 with step of 10), maximum number of attributes (from 4 to 10), use of bootstrapping (true or false)
- Neural network, hyperparameters: number of hidden layers, with one or two layers and varied number of neurons in the hidden layers (minimum of 4, maximum of 20).

Analyses were also performed assuming the availability of various measurement channels, which would simplify the diagnostic system for assessing tool conditions. Table 4 shows the comparisons that were made and presents the best models obtained using the k-fold CV test for the given data set, as well as the results obtained during testing for the test set (weighted accuracy, precision, recall, F1). The table shows the results for all available channels, for the measuring point on the clamp, and for the

Table 4. Results of tests for different subsets of features

Signal source and applied preprocessing	The best model based on performance on the train set	Results for test set			
		Weighted accuracy	Precision	Recall	F1
All channels (sensors on clamp and spindle, both directions), measures based on original signals and information about the speed of the cutting process	KNN classifier city-block distance metric, k = 3	0.992	0.996	0.991	0.979
All channels (as above), measures calculated after applying the SSA transformation and information about the speed of the cutting process	KNN classifier city-block distance metric, k = 3	0.980	0.974	0.966	0.970
All channels (as above), measures calculated based on bands displayed in Table 3 and information about the speed of the cutting process	KNN classifier city-block distance metric, k = 7	0.999	0.991	1.000	0.996
Measurements only on the clamp, measures based on the original signals, without the information about the speed of the cutting process	Random forrest, maximum number of attributes: 5, number of decision trees: 50.	0.971	0.973	0.948	0.960
Measurements on the clamp, measures calculated after applying the SSA transformation without the information about the speed of the cutting process	KNN classifier city-block distance metric, k = 7	0.953	0.924	0.924	0.924
Measurements on the clamp, measures calculated based on bands displayed in Table 3 without the information about the speed of the cutting process	KNN classifier city-block distance metric, k = 1	0.985	0.982	0.973	0.978
Measurements on the spindle, measures based on the original signals without the information about the speed of the cutting process	KNN classifier city-block distance metric, k = 4	0.986	0.991	0.974	0.982
Measurements on the spindle, measures calculated after applying the SSA transformation without the information about the speed of the cutting process	KNN classifier city-block distance metric, k = 3	0.971	0.934	0.958	0.946
Measurements on the spindle, measures calculated based on bands displayed in Table 3 without the information about the speed of the cutting process	KNN classifier city-block distance metric, k = 3	0.993	0.974	0.991	0.982

measuring point on the spindle. In the part of analyses whose results are presented in Table 4 the cutting speed v_c was not taken into account, which significantly simplifies the measuring system. The v_c parameter when added by the human operator, can be prone to error which is why the diagnostic should not require it for the assessment of tool wear.

In these tables, the results are presented with weighted accuracy as the average accuracy across both classes. This measure seems more appropriate due to the uneven number of class representatives (338 for usable condition and 73 for unusable).

Classification quality measures were calculated according to the following formulas:

- weighted accuracy

$$oa_w = 1 - \frac{1}{K}\sum_{i=1}^{K} \frac{n_{Fi}}{n_i} \tag{5}$$

where: K – number of classes, number of false classifications for class i, the total number of examples in a class I.

- precision

$$Prec = \frac{TP}{TP + FP} \tag{6}$$

where: TP – number of true positives classifications, FP – number of false positives classifications.

- recall

$$Rec = \frac{TP}{TP + FN} \tag{7}$$

where: FN – number of false negatives classifications.

- score F1

$$F_1 = \frac{2 \cdot Prec \cdot Rec}{Prec + Rec} \tag{8}$$

For the analyzed data, the k-nearest neighbors method often proved to be the best classification method in our investigations. Mostly, classifiers with a small value of the parameter k were selected, which indicates a fairly complex data structure and the crucial importance of local dependencies in the feature space. The best classifier was built based on signals from both measuring points and both directions. It also took into account information about the cutting speed. The accuracy obtained on its basis was 0.999 and the failure detection efficiency (in the test data set) was 100%. However, this model is difficult to implement in practice because it requires entering information about the cutting speed into the diagnostic system and the location of the measuring point on both the clamp and the spindle. Placing the vibration sensor on the clamp, in the working space of the tools, is troublesome in industrial conditions. It seems possible to simplify the measurement system by selecting just one point. It turns out that, for the material in question, the best point is on the spindle, rather than on the clamp. This suggests that, despite the spindle measurement being affected by vibrations generated by the spindle itself, the excitations from the cutting process produce measurable responses on the spindle. A significant difficulty that may worsen the measurement results on the clamp is the variable distance of the sensor from the contact point of the tool and material. Different frequency bands may be attenuated differently with changing

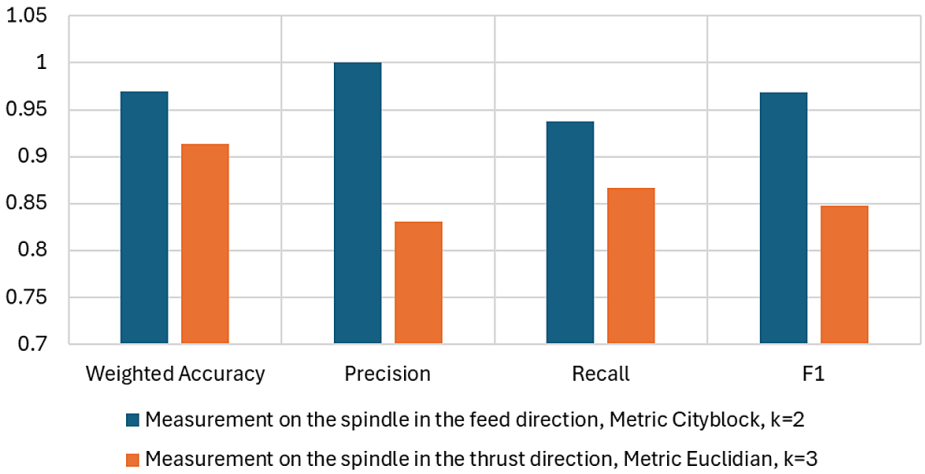

Figure 20. Results of quality measures of the classifier, after including the information from only one of the measured directions

distance from the source to the sensor, leading to greater variability in measurement conditions. The reference analysis presented in Table 4 shows that the information about cutting speed is not necessary either to develop a reliable tool condition diagnosis. At the cost of a slight decrease in classification quality (accuracy 0.993 and probability of detecting an unfit state 0.991) the system can be simplified significantly. Unfortunately, this is associated with an increase in the number of false alarms regarding tool wear (precision 0.974). Further comparisons of results indicate a clear benefit from filtering the signal. For example, for measurements obtained only from a point located on the spindle and without information about the cutting speed without signal filtering, the accuracy of the model drops from 0.993 to 0.986. The nature of the errors made by the classifier also changes. It will put out fewer false alarms, but it will ignore the unfit state to a greater extent. Thanks to filtering, the signal bands with the highest information value are distinguished, which increases the sensitivity to changes in the state of individual signal measures. Including measures from the most informative components obtained through SSA worsens the quality of predictions. Including three components results in too much information loss. Results are difficult to generalize to other processed materials, tools, or machines with different designs, but they can be seen as important as they show the potential for developing an effective diagnostic system based on simple measures of filtered signal bands obtained from a sensor directly mounted on the spindle. Figure 20 presents classification results for the test set related to further attempts to simplify the diagnostic system by using only one measurement direction from the sensor mounted on the spindle and filtered signal bands.

CONCLUSIONS

Simple methods of tool condition analysis based on basic measures of the vibration signal (e.g. the RMS value of the signal) may prove insufficient to determine the condition of the tool with satisfactory accuracy. Hence, it is necessary to reach for models that take into account many measures simultaneously, which allows for increasing the reliability of inference. For this purpose, many models with different hyperparameter values should be developed and the results of inference based on a separate test set should be compared. Thanks to such methods, it was possible to build a model that allows for obtaining inference accuracy at a level of almost 100%. Despite the existence of such a possibility, from a practical point of view, a compromise between accuracy and possibilities of industrial applications is necessary. Therefore, a simplified model was finally proposed, based only on the registration of vibrations on the spindle. Although this point is further from the source and can be disturbed by the spindle drive, it turns out to be better in terms of distinguishing states. Additionally, it seems advisable to use a model that does not require operator intervention, and therefore does not take into account information about the cutting speed. Such a model, based on k-NN method, was built with an accuracy of 99.3% for the test set, which allows for the detection of over 99% of tool damage cases. This is the model we consider useful in practice. To sum up, the following conclusions can be drawn:

- The applied machine learning method allows for the elimination of cutting speed v_c from the tool condition assessment process, as well as the tool's operational time, simplifying the diagnostic system to an easily automatable measurement of vibration accelerations on the spindle.
- The best results were achieved through bandpass filtering of the signal. Frequency selection enhances the sensitivity of individual measures by reducing the impact of phenomena that can introduce noise into the diagnostic signal.
- Analysis based on a subset of components obtained via SSA did not meet expectations.
- The results obtained for the test set suggest that the optimal measurement point in the problem under consideration is the spindle, even though theoretically this point might have other sources of vibrations, and the signal path from the source to the sensor is more "complex." The results achieved exhibit very high accuracy.
- When using signal filtering, a classifier with relatively high sensitivity and lower precision was developed, which may lead to relatively more false alarms and premature tool changes. Of course, whether the classifier should "prefer" high sensitivity or precision depends on the user's policy for the diagnostic system. If the cost of false negatives is greater than that of false positives, the model should be selected to favor higher sensitivity.

Although the results are difficult to generalize to other cases, they are important as they demonstrate the potential for building an effective diagnostic system based on simple measures of filtered signal bands obtained from a sensor, for example, directly mounted on the spindle.

REFERENCES

1. Zhou Y, Xue W. Review of tool condition monitoring methods in milling processes. Int J Adv Manuf Technol. 2018 May; 96(5–8): 2509–23. https://doi.org/10.1007/s00170-018-1768-5
2. Pimenov DYu, Kumar Gupta M, Da Silva LRR, Kiran M, Khanna N, Krolczyk GM. Application of measurement systems in tool condition monitoring of Milling: A review of measurement science approach. Measurement. 2022 Aug; 199: 111503. https://doi.org/10.1016/j.measurement.2022.111503
3. Patra K, Jha AK, Szalay T, Ranjan J, Monostori L. Artificial neural network based tool condition monitoring in micro mechanical peck drilling using thrust force signals. Precision Engineering. 2017 Apr; 48: 279–91. https://doi.org/10.1016/j.precisioneng.2016.12.011
4. Huang PB, Ma CC, Kuo CH. A PNN self-learning tool breakage detection system in end milling operations. Applied Soft Computing. 2015 Dec; 37: 114–24. https://doi.org/10.1016/j.asoc.2015.08.019
5. Ratava J, Lohtander M, Varis J. Tool condition monitoring in interrupted cutting with acceleration sensors. Robotics and Computer-Integrated Manufacturing. 2017 Oct; 47: 70–5. https://doi.org/10.1016/j.rcim.2016.11.008
6. Navarro-Devia JH, Chen Y, Dao DV, Li H. Chatter detection in milling processes—a review on signal processing and condition classification. Int J Adv Manuf Technol. 2023 Apr; 125(9–10): 3943–80. https://doi.org/10.1007/s00170-023-10969-2
7. M Lamraoui, M Thomas, M El Badaoui. Cyclostationarity approach for monitoring chatter and tool wear in high speed milling. Mechanical Systems and Signal Processing. 2014; 44(177–198). https://doi.org/10.1016/j.ymssp.2013.05.001
8. Twardowski P, Tabaszewski M, Wiciak – Pikuła M, Felusiak-Czyryca A. Identification of tool wear using acoustic emission signal and machine learning methods. Precision Engineering. 2021 Nov; 72: 738–44. https://doi.org/10.1016/j.precisioneng.2021.07.019
9. Filippov AV, Rubtsov VE, Tarasov SYu. Acoustic emission study of surface deterioration in tribocontacting. Applied Acoustics. 2017 Feb; 117: 106–12. https://doi.org/10.1016/j.apacoust.2016.11.007
10. Kishawy HA, Hegab H, Umer U, Mohany A. Application of acoustic emissions in machining processes: analysis and critical review. Int J Adv Manuf Technol. 2018 Sep; 98(5–8): 1391–407. https://doi.org/10.1007/s00170-018-2341-y
11. Jessel T, Byrne C, Eaton M, Merrifield B, Harris S, Pullin R. Tool condition monitoring of diamond-coated burrs with acoustic emission utilising machine learning methods. Int J Adv Manuf Technol. 2024 Jan; 130(3–4): 1107–24. https://doi.org10.1007/s00170-023-12700-7
12. Ren Q, Balazinski M, Baron L, Jemielniak K, Botez R, Achiche S. Type-2 fuzzy tool condition monitoring system based on acoustic emission in micromilling. Information Sciences. 2014 Jan; 255: 121–34. https://doi.org/10.1016/j.ins.2013.06.010
13. Pimenov DY, Bustillo A, Wojciechowski S, Sharma VS, Gupta MK, Kuntoğlu M. Artificial intelligence systems for tool condition monitoring in machining: analysis and critical review. J Intell Manuf. 2023 Jun; 34(5): 2079–121. https://doi.org/10.1007/s10845-022-01923-2
14. Serin G, Sener B, Ozbayoglu AM, Unver HO. Review of tool condition monitoring in machining and opportunities for deep learning. Int J Adv Manuf Technol. 2020 Jul; 109(3–4): 953–74. https://doi.org/10.1007/s00170-020-05449-w
15. Ngo T. Data mining: practical machine learning tools and technique, third edition by Ian H. Witten, Eibe Frank, Mark A. Hell. SIGSOFT Softw Eng Notes. 2011 Sep 30; 36(5): 51–2. https://doi.org/10.1145/2020976.2021004
16. Sick B. On-line and indirect tool wear monitoring in turning with artificial neural networks: a review of more than a decade of research. Mechanical Systems and Signal Processing. 2002 Jul; 16(4): 487–546. https://doi.org/10.1006/mssp.2001.1460
17. Kuntoğlu M, Aslan A, Sağlam H, Pimenov DY, Giasin K, Mikolajczyk T. Optimization and analysis of surface roughness, flank wear and 5 different sensorial data via tool condition monitoring system in turning of AISI 5140. Sensors. 2020 Aug 5; 20(16): 4377. https://doi.org/10.3390/s20164377
18. Tabaszewski M, Twardowski P, Wiciak-Pikuła M, Znojkiewicz N, Felusiak-Czyryca A, Czyżycki J. Machine learning approaches for monitoring of tool wear during grey cast-iron turning. Materials. 2022 Jun 20; 15(12): 4359. https://doi.org/10.3390/ma15124359
19. Mohanraj T, Shankar S, Rajasekar R, Sakthivel NR, Pramanik A. Tool condition monitoring techniques in milling process — a review. Journal of Materials Research and Technology. 2020 Jan; 9(1): 1032–42. https://doi.org/10.1016/j.jmrt.2019.10.031
20. Twardowski P, Czyżycki J, Felusiak-Czyryca A, Tabaszewski M, Wiciak-Pikuła M. Monitoring and

forecasting of tool wear based on measurements of vibration accelerations during cast iron milling. Journal of Manufacturing Processes. 2023 Jun; 95: 342–50. https://doi.org/10.1016/j.jmapro.2023.04.036

21. Pandiyan V, Shevchik S, Wasmer K, Castagne S, Tjahjowidodo T. Modelling and monitoring of abrasive finishing processes using artificial intelligence techniques: A review. Journal of Manufacturing Processes. 2020 Sep; 57: 114–35. https://doi.org/10.1016/j.jmapro.2020.06.013
22. Huang Z, Zhu J, Lei J, Li X, Tian F. Tool wear predicting based on multi-domain feature fusion by deep convolutional neural network in milling operations. J Intell Manuf. 2020 Apr; 31(4): 953–66. https://doi.org/10.1007/s10845-019-01488-7
23. Geron A. Hands -On Machine Learning with Scikit-Learn and TensorFlow, O'Reilly Media, 2019.
24. Kornacki J., Ćwik J. Statystyczne systemy uczące się, WNT, Warszawa 2005 (in Polish)
25. Larose D. Discovering Knowledge in Data, An Introduction to Data Mining, John Wiley & Sons, Inc. 2005.
26. Tool steel WNLV/1.2714/55NiCrMoV7 chemical composition: https://akrostal.pl/en/stale/wnlv-1-2714-55nicrmov7/
27. Cempel C. Vibroacoustic Condition Monitoring, Ellis Horwood, London, 1991
28. Bonizzi P, Karel JMH, Meste O, Peeters RLM. Singular spectrum decomposition: a new method for time series decomposition. Adv Adapt Data Anal. 2014 Oct; 6(4): 1450011. https://doi.org/10.1142/S1793536914500113
29. Alexandrov T. Method of Trend Extraction Using Singular Spectrum Analysis. REVSTAT-Statistical Journal. 2009 Apr 28; 1–22. https://doi.org/10.48550/arXiv.0804.3367
30. Borodich Suarez S, Heravi S, Pepelyshev A. Forecasting industrial production indices with a new singular spectrum analysis forecasting algorithm. Statistics and Its Interface. 2023; 16(1): 31–42. https://doi.org/10.4310/SII.2023.v16.n1.a3